



Published in final edited form as:

Neurobiol Dis. 2021 January ; 148: 105222. doi:10.1016/j.nbd.2020.105222.

Sex specific correlation between GABAergic disruption in the dorsal hippocampus and flurothyl seizure susceptibility after neonatal hypoxic-ischemic brain injury

Charles R. Lechner^{a,1}, Melanie A. McNally^{b,1}, Mark Pierre St.^a, Ryan J. Felling^b, Frances J. Northington^a, Carl E. Stafstrom^b, Raul Chavez-Valdez^{a,*}

^aDivision of Neonatology, Department of Pediatrics, Johns Hopkins University School of Medicine, 600 North Wolf Street, Baltimore, MD 21287, USA

^bDepartment of Neurology, Johns Hopkins University School of Medicine, 600 North Wolf Street, Baltimore, MD 21287, USA

Abstract

Since neonatal hypoxia-ischemia (HI) disrupts the hippocampal (Hp) GABAergic network in the mouse and Hp injury in this model correlates with flurothyl seizure susceptibility only in male mice, we hypothesized that GABAergic disruption correlates with flurothyl seizure susceptibility in a sex-specific manner. C57BL6 mice were exposed to HI (Vannucci model) versus sham procedures at P10, randomized to normothermia (NT) or therapeutic hypothermia (TH), and subsequently underwent flurothyl seizure testing at P18. Only in male mice, Hp atrophy correlated with seizure susceptibility. The number of Hp parvalbumin positive interneurons (PV⁺INs) decreased after HI in both sexes, but TH attenuated this deficit only in females. In males only, seizure susceptibility directly correlated with the number of PV⁺INs, but not somatostatin or calretinin expressing INs. Hp GABA_B receptor subunit levels were decreased after HI, but unrelated to later seizure susceptibility. In contrast, Hp GABA_A receptor α 1 subunit (GABA_AR α 1) levels were increased after HI. Adjusting the number of PV⁺INs for their GABA_AR α 1 expression strengthened the correlation with seizure susceptibility in male mice. Thus, we identified a novel Hp sex-specific GABA-mediated mechanism of compensation after HI that correlates with flurothyl seizure susceptibility warranting further study to better understand potential clinical translation.

This is an open access article under the CC BY-NC-ND license (<http://creativecommons.org/licenses/by-nc-nd/4.0/>).

*Corresponding author at: Department of Pediatrics, Division of Neonatology, Johns Hopkins Hospital, 600 N. Wolfe Street, CMSC 6-104 Baltimore, MD 21287, USA. rchavez2@jhmi.edu (R. Chavez-Valdez).

¹These authors contributed equally to the study and are considered co-first authors.

Author Contributions

All authors had full access to all the data in the study and take responsibility for the integrity of the data and the accuracy of the data analysis. Contributions: RC-V, MAM, FJN, RJF, and CES in conception; RC-V, MAM, CRL, FJN, and CES in design; RC-V, CRL, MAM, and MSP in acquisition of data and analysis, RC-V, MAM, CRL, MSP, RJF, FJN, and CES in data interpretation, RC-V, CRL, and MAM in drafting of manuscript; and RC-V, FJN, MAM, RJF and CES in funding acquisition. All authors have critically reviewed the final manuscript for important intellectual content and have given their final approval for publication

Disclosure/Conflict Of Interest

We confirm that there are no known conflicts of interests associated with this publication and there has been no significant financial support for this work that could have influenced its outcome

Appendix A. Supplementary data

Supplementary data to this article can be found online at <https://doi.org/10.1016/j.nbd.2020.105222>.

Keywords

GABA receptor; Neonatal seizure; Parvalbumin; Sex-dimorphism; Somatostatin; Neonatal brain injury; Hypoxic-ischemic brain injury

1. Introduction

Hypoxic-ischemic brain injury (HI) is common in the newborn period, complicating 2–6/1000 live term births worldwide (Kurinczuk et al., 2010; Shetty, 2015). Despite generalized use of therapeutic hypothermia (TH), nearly half of all patients die or develop severe neurodevelopmental disability (Azzopardi et al., 2009; Pfister and Soll, 2010). HI is also the most common cause of neonatal seizures, with 40–60% of neonates with HI developing electrographic seizures in the first few days of life (Boylan et al., 2015; Glass et al., 2014). Whether neonatal seizures cause additive harm after HI or are just a biomarker of severe injury remains an area of active research. Small clinical studies demonstrate that electrographic seizure burden correlates with degree of brain injury on MRI regardless of initial clinical severity or aEEG background (Shah et al., 2014). Treating electrographic seizures decreases seizure burden (Srinivasakumar et al., 2015) and lower seizure burden is associated with better long term neurodevelopmental outcomes (Glass et al., 2009; McBride et al., 2000; Srinivasakumar et al., 2015; Toet et al., 2005). However, there is no definitive evidence that treating post-HI neonatal seizures improves developmental outcomes. Moreover, available first line agents, such as phenobarbital, phenytoin, and benzodiazepines, control fewer than half of neonatal seizures (Glass et al., 2019; Painter et al., 1999; Van Rooij et al., 2013) and can exert adverse effects and may cause neuronal apoptosis in the developing brain (Bittigau et al., 2003; Sulzbacher et al., 1999). Thus, current treatments for post-HI neonatal seizures are not sufficiently effective and may be potentially harmful. Due to the questions of treatment efficacy, side effects, and long-term impact, there remains equipoise regarding ideal treatment strategy for managing neonatal seizures in neonates with HI (Hellström-Westas et al., 2015; McNally and Hartman, 2017). To optimize treatment and prioritize future research efforts, a better understanding of the pathophysiology of neonatal seizures following HI in the developing brain is paramount.

Gamma-aminobutyric acid (GABA) is the main inhibitory neurotransmitter in the central nervous system and the target of most commonly used anti-seizure drugs for neonatal seizures after HI (Bassan et al., 2008; Clancy, 2006). In the developing brain, GABAergic receptors, synthetic enzymes, and neurons are actively undergoing changes that are age, region, and sex dependent (Galanopoulou, 2008; Giorgi et al., 2014; Luhmann et al., 2014; Schwenk et al., 2016). The understanding of how neonatal HI disrupts the developing GABAergic system is incomplete. Elucidating these specifics may identify mechanisms underlying anti-seizure drug ineffectiveness, seizure susceptibility, and long-term adverse neurodevelopmental outcomes.

Previous work from our lab has demonstrated that, even with TH treatment, neonatal HI results in decreased numbers of parvalbumin (PV) expressing interneurons (INs), the most abundant GABAergic interneuron in the brain (Chavez-Valdez et al., 2018; Goffigan-Holmes

et al., 2019). We additionally showed simplification of GABAergic dendritic arbors and decreased expression of the GABA synthetic enzymes GAD65/67 in the mouse hippocampus after neonatal HI (Chavez-Valdez et al., 2018; Goffigan-Holmes et al., 2019). Using the inhalant convulsant flurothyl, a GABA_A receptor (GABA_AR) antagonist, we have also shown that seizure susceptibility in the same model correlates with hippocampal injury in male mice and is not mitigated by TH (McNally et al., 2019). Thus, experimental TH provides incomplete protection against hippocampal injury, flurothyl seizure susceptibility, and GABAergic disruption in mice after HI. Interestingly, while the loss of PV⁺INs in the hippocampus after neonatal HI is independent of sex, seizure susceptibility in this model at the same experimental time (8 days after the insult) is not (Chavez-Valdez et al., 2018; McNally et al., 2019). Therefore, we hypothesize that the relationship between GABAergic disruption and flurothyl seizure susceptibility after neonatal HI in the mouse is sex-specific.

2. Materials and methods

2.1. Animals

A total of 53 C57BL6 mice of both sexes (30 males and 23 females) that underwent flurothyl seizure susceptibility testing were used for experiments. A ~ 20% mortality rate, similar in both sexes, was observed while generating these mice. Approval for the animal protocol was granted by the Institutional Animal Care and Use Committee at Johns Hopkins University School of Medicine and followed the Guide for the Care and Use of Laboratory Animals provided by the NIH, US Department of Health and Human Services 85–23, 1985. ARRIVE guidelines (g.uk/arrive-guidelines) were also followed.

2.2. Neonatal hypoxic-ischemic brain injury and therapeutic hypothermia

In 41 mice at postnatal day (P)10, a modified Vannucci model was used to induce HI as previously described (Diaz et al., 2017; Graham et al., 2004). Pups were anesthetized with isoflurane (induction at 3% and maintenance at 1%) followed by unilateral ligation of the right carotid artery. Pups were exposed to isoflurane for 3–5 min, including the isoflurane induction for 30 s. After the ligation surgery, pups were given a 1-h recovery period with the dam. Following the recovery period, pups were exposed to 45 min of hypoxia (FiO₂, 0.08). As done in previous studies, after the hypoxia exposure the pups were randomized to normothermia (NT, 36 °C, 22 mice) or TH (31 °C, 19 mice) treatment for 4 h (Burnsed et al., 2015; Diaz et al., 2017; Goffigan-Holmes et al., 2019). Treatment temperatures were monitored via rectal measurements that were performed in one pup per treatment group with the use of a tissue implantable thermocouple microprobe and the PowerLab data acquisition system (Ad Instruments, Inc., Colorado Springs, CO). To generate control shams, 12 pups were exposed to anesthesia for 5 min. Following the 1-h dam recovery period, control sham pups were kept away from the dam and their temperature was monitored and maintained at 36 °C for 4 h. After the 4-h treatments ended, all pups were returned to the dam. Flurothyl seizure susceptibility was tested at P18, 8 days after HI (see section below), following which mice of both sexes were euthanized and perfused. The one-drop exposure method (Markovic and Murasko, 1993) was used to anesthetize mice using a 20% (v/v) mixture of isoflurane in propylene glycol. Exsanguination was performed intracardially using 10 mM PBS (pH 7.4) and 4% paraformaldehyde in 0.1 M phosphate buffer to fix the brains. Brains were then

cryoprotected using 30% sucrose in PBS. These perfused brains were used for immunohistochemistry (IHC) while other brains were gathered as unfixed fresh tissue to be used in western blots (WB) to validate antibodies for IHC use.

2.3. Flurothyl Seizure Susceptibility Testing

Pups were exposed to flurothyl for seizure susceptibility at P18 as previously described (McNally et al., 2019). Flurothyl acts as a GABA_AR antagonist and causes convulsions when inhaled. Flurothyl is not metabolized and the evoked seizures are generalized in a body weight independent manner (Prichard et al., 1969). Flurothyl ether (Synquest Laboratories, Alachua, FL) was dripped from the top of a 30 × 30 × 24 cm plexiglass chamber at a rate of 40 µL/min onto a piece of filter paper (separated from the pup) at the base of the chamber. Times to seizure stages were recorded: loss of posture (initial timepoint measured, approximates a stage 3 seizure (S3)(Racine, 1972)) and tonic hindlimb extension (final timepoint measured, approximates a stage 5 seizure (S5) (Racine, 1972)).

2.4. Western blotting and Nissl staining

Crude brain homogenates, including the hippocampus, were prepared at P18 to validate the antibodies used in IHC, as we previously reported (Chavez-Valdez et al., 2020). In brief, homogenates were cryoprotected by the addition of 20% (*w/v*) glycerol, protein concentrations were determined by Bradford assay (Bradford, 1976), and 25 µg of protein homogenate diluted 3:1 (*v:v*) with 4× loading buffer (reducing conditions) were used for WB. Homogenates were loaded into 4–20% mini-protean TGX polyacrylamide precast protein gels (Biorad Inc., Hercules, CA) and then transferred to nitrocellulose membrane using TransBlot Turbo Midi-size (Biorad Inc). Membranes were blocked with 2% normal goat serum (NGS) in 0.1% Tween/TBS (TBS-T) to replicate IHC experimental conditions. Following overnight exposure with primary antibodies at 1:1000 at 4 °C and washes with TBS-T, membranes were exposed to secondary antibodies for 1 h. Enhanced chemiluminescence (Clarity Western ECL Substrate, Biorad Inc.) was used to develop the membranes after secondary exposure. To verify that the suitability of the primary antibody for immunofluorescence (IF)-IHC, the antibody must produce a single band or multiple bands at molecular weight(s) well described for the targeted proteins, with no non-specific binding detected. Exceptions were made for well-reported post-transcriptional modifications that are also detected with the antibody.

2.5. Floating IF IHC

After cryoprotection via immersion in 30% sucrose in PBS solutions, perfused brains were flash-frozen using 2-methylbutane and stored at – 80 °C. A freezing microtome was used to cut the brains coronally into 50 µm sections. Injury assessment was performed using Nissl counterstaining and a glial fibrillary acidic protein (GFAP)-derived scoring system, as described below (Chavez-Valdez et al., 2018). Tissue sections were washed in TBS pH 7.2 for 10 min before antigen retrieval with sodium citrate buffer pH 6.0 for 90 min at 80 °C. *triton X* (0.4%) in TBS was used for 15 min to permeabilize the tissue followed by blocking using 10% NGS in 0.1% Tween/TBS for 1 h at room temperature. Sections were then exposed to the following primary antibodies: i) chicken anti-parvalbumin (PV, Novus Biological LLC, Centennial, CO; 1:250), ii) rabbit anti-somatostatin (SST, Genetex Inc.,

Irvine, CA; 1:400), iii) rabbit anti-calretinin (CAL, Abcam PLC, Cambridge, MA; 1:250), or mouse anti-CAL (ProteinTech Inc., Rosemont, IL; 1:250), iv) mouse anti-GABA_A α 1 subunit (StressMarq Inc., Victoria, British Columbia; 1:400), or rabbit anti-GABA_A α 1 subunit (Thermo Fisher Scientific Inc., Waltham MA; 1:400), v) mouse anti-GABA_B R1 (Abcam PLC; 1:400) and vi) rabbit anti-GABA_B R2 (Abcam PLC; 1:400). Primary antibodies were diluted with 4% NGS in either TBS (GABA_A α 1, GABA_B R1, GABA_B R2) or TBS-T (PV, SST, CAL) overnight at 4 °C. After incubation with primary antibodies, sections were exposed for 2 h in the dark at room temperature in a 4% NGS/TBS-T solution with species and subtype-specific cross-absorbed secondary antibodies conjugated to either Alexa Fluor 488, Alexa Fluor 568, or Alexa Fluor 647, emitting green, red, or deep red fluorescence signal respectively (Thermo Fisher Scientific, Inc). Tissues were also incubated for 5 min in 4',6-diamidino-2-phenylindole (DAPI, 1 μ g/mL) in TBS after secondary antibody incubation. Tissues were then washed in TBS, mounted, and dried for 30 min before being coverslipped with ProLong Glass Antifade Mountant (Molecular Probes, Life Technologies Corp., Carlsbad, CA).

2.6. Antibodies

All antibodies used in IF-IHC experiments were tested for specificity in western blots as described above. To ascertain specificity of immunostaining, all experiments were run with negative controls, which included sections exposed to no primary antibody or to species and subtype specific immunoglobulin at similar concentrations (μ g/ mL) to those use for primary antibodies. Sections used for negative controls were chosen from brains showing the strongest immunoreactivity to antibodies deemed to be specific to protein targets. Further, to ensure specificity of mouse antibodies, blocking step was incorporated after standard 10% NGS using Goat F(ab) polyclonal secondary antibody to mouse IgG in excess (Abcam PLC, 1:25) for 90 min. A list of the tested primary antibodies, as well as the species and subtype-specific immunoglobins used for negative controls, are detailed (Supplemental table 1).

2.7. Histopathologic Injury Scoring

Two different hippocampal scoring systems were used to grade injury by two independent sets of blinded researchers. The first system used was based on a previously published grading scale (Sheldon et al., 2004), where hippocampal injury scores ranged from 0 to 9 based on a visual inspection of the Nissl stained, coronally cut, sequential brain slices (MAM and FJN). This assessment included the Cornu Ammonis (CA) 1, CA3, and dentate gyrus (DG) subregions of the entire hippocampus. The second hippocampal injury scoring was based on the inspection of GFAP IHC focused on immunoreactivity, presence of glial scars, astrocyte body size, abundance, thickness of branching and overlapping of domains (RCV), previously reported (Chavez-Valdez et al., 2018). This second scoring system was used to corroborate the results obtained for the visual inspection of Nissl counterstained slices. Correlation between these two systems in our hands has been previously published (McNally et al., 2019).

2.8. Semi-quantitative Hippocampal Atrophy Assessment

Several studies link neonatal HI brain injury, hippocampal atrophy (Annink et al., 2019; Gadian et al., 2000), and neonatal seizures (Boylan et al., 2015; Glass et al., 2014).

Although, the directionality of these relationships is still debatable, the potential role of hippocampal atrophy in seizure susceptibility needs to be taken into account. Both scoring systems described above focus on the assessment of the pyramidal cell (PCL) and the granular cell (GCL) layers containing cell bodies, but provide little assessment of the neuropil, which represents the largest portion of hippocampal volume containing axons, dendrites and glial processes forming the synapses (Mishchenko et al., 2010). Therefore, we also evaluated injury using a semi-quantitatively assessment of hippocampal atrophy, as we have previously reported (Goffigan-Holmes et al., 2019). We extrapolated measurements of right (HI injured) hippocampal volumes and percent of residual hippocampal volume when compared to the left (contralateral – hypoxia exposed) hippocampal volume. Hippocampal volumes were calculated using the area (mm²) obtained from 5 sequential 50 µm thick, cresyl violet-stained coronal brain sections positioned 600 µm apart in the anteroposterior axis of the brain at P18. Total residual volume was extrapolated using the following formula:

$$\text{Hippocampal volume (mm}^3\text{)} = \sum_{i=1}^{(n=5)} [S_i * 0.05] + \sum_{i=1}^{(n=4)} [(S_i + S_{i+1}) * 0.6/2].$$

where, i = coronal section position in the antero-posterior axis, n = number of sum repeats, and.

S = hippocampal area in mm² (Fig. 1).

These results closely mirror our previous assessment of hippocampal volumes using T2W MRI in the same model (Burnsed et al., 2015).

2.9. Quantification of IHC

Anterior coronal brain sections were used to evaluate the dorsal CA1 and CA3 subfields of the hippocampus. The boundaries of the dorsal hippocampus with the antero-posterior axis have been previously defined (Chavez-Valdez et al., 2020). The dorsal CA1 analysis included the region limited by the subiculum (septally) and the CA2 subfield (temporally). The dorsal CA3 analysis included the region limited by the CA2 subfield and the polymorph cell layer of the DG hilus. The analysis was performed primarily in the PCL of the dorsal CA1 and CA3 subfields, except for evaluation of SST IF, which showed the soma of INs mostly located in the oriens layer (OrL) with extension to the PCL in transit to the lacunosum-moleculare layer.

2.10. Quantification of dorsal area

CA1 and CA3 areas were measured using the freehand selection function of ImageJ software (NIH, Bethesda, MD) and calibrated to mm².

2.11. Quantification of percent area of IF

Images were taken at 2048 × 2048 pixels, 16 bit depth, and averaged x2, captured using a 20×/0.8 objective and 1.0 zoom to produce uncompressed images of 320 µm². The average of the z-stack images taken at 3 to 4 planes of the section were averaged. Percent area of immunostaining was determined by calculating the area of IF using the threshold function in

ImageJ software relative to the total area of the CA1 or CA3 PCL (or PCL/OrL for SST analysis) within the image.

2.12. Quantification of number of PV⁺ and SST⁺ INs

Z-stacks were taken with the same specification described above to produce an uncompressed image of 320 μm^2 presenting the entire CA1 and CA3 subfields. Following 3D reconstruction, the number of PV⁺ and SST⁺ neurons was calculated relative to the evaluated area.

2.13. Statistics

The aim of the study was not to assess sex differences, but instead to evaluate the response to therapies by sex. Data failed Shapiro-Wilks analysis of normality, thus non-parametric Kruskal-Wallis one-way ANOVA was applied stratified by sex, along with Dunn-Bonferroni's post-hoc test. Box and whisker plots, where the box is limited by the 25th and 75th percentiles and the solid line represents the median, were used to present the results. In all cases significance was assigned by p -value < 0.05 . Non-parametric Spearman Rho correlations were applied and a best-fit regression line was calculated. IBM SPSS Statistics 24v (IBM Corporation, Armonk, NY) was used to perform all of the analysis.

3. Results

TH attenuates hippocampal atrophy 8 days after HI and correlates with seizure susceptibility in male mice. Hippocampal volume was 26.4% smaller in NT mice than in sham mice (KW ANOVA $p = 0.001$; $p = 0.001$ vs. sham; Fig 1A₁). After stratification by sex, hippocampal volume was 32.5% smaller in NT male mice (KW ANOVA $p = 0.025$; $p = 0.021$ vs. sham) and 20.4% smaller in NT female mice (KW ANOVA $p = 0.023$; $p = 0.026$ vs. sham, Fig 1A₂). Although hippocampal volumes were still smaller in TH-treated mice than shams (-17.4% , $p = 0.015$; Fig 1A₁), when sex-stratified TH did attenuate hippocampal atrophy in male mice (Fig 1A₂). We found no difference in body weight between male and female mice at P10 or P18 (Mann-Witney U test). However, NT female mice were $\sim 15\%$ smaller than shams (KW ANOVA $p = 0.024$, $p = 0.032$ vs. sham, data not shown). Thus, to account for the sexual dimorphism in body weight 8 days after HI injury and the potential effect of hypoxia exposure in the described right hippocampal atrophy, we also calculated residual volumes relative to contralateral hippocampus (left). Residual volume was 31.5% smaller in NT mice than in sham mice (KW ANOVA $p < 0.001$; $p < 0.001$ NT vs. sham; Fig 1B₁). Stratified by sex, hippocampal residual volumes were 31.1% and 21.3% smaller in NT male (KW ANOVA $p = 0.020$; $p = 0.018$ vs. sham) and female mice (KW ANOVA $p = 0.023$; $p = 0.028$ vs. sham, Fig 1B₂), respectively. Similar to right hippocampal atrophy, TH attenuated the decrease in residual volumes only in male injured mice 8 days after HI.

Because multiple cellular components may account for hippocampal atrophy, we next evaluated how hippocampal volumes related to histologic injury. The correlation between hippocampal atrophy and histological scoring of hippocampal injury was not linear (Fig 1A₃ and 1B₃). Hippocampal volumes or residual volumes became smaller only after the histological scores were at least 6 out of 9 (inflexion point) 8 days after HI. Representative

photomicrographs of a sham and a NT treated mouse are shown to illustrate these findings (Fig. 1C). We have previously reported an inverse correlation between histological scores and flurothyl seizure susceptibility by 8 days after HI injury in male mice (McNally et al., 2019). Thus, we assessed if volumetric analysis also related to latency to seizure stages S3 and S5. Both hippocampal volumes and residual volumes correlated directly with latency to S5 in male mice and these correlations were stronger than reported for histological scores previously ($R^2 = 0.49$, $p < 0.001$, Fig. 1D and E) (McNally et al., 2019).

The number of PV + INs correlates with flurothyl seizure susceptibility and hippocampal residual volume in a sex-specific manner. Eight days after neonatal HI, the number of PV⁺INs was decreased in the dorsal CA1 PCL by 51% (KW ANOVA $p = 0.004$; $p = 0.008$ vs. sham; Fig. 2A) and in CA3 PCL by 37% (KW ANOVA $p = 0.02$; $p = 0.04$ vs. sham; Fig. 2B) in male mice. Similarly, PV⁺INs decreased in CA1 PCL by 71% ($p = 0.007$ vs. sham; Fig. 2A) and in CA3 PCL by 45% ($p = 0.04$ vs. sham; Fig. 2B) in female mice. No change in the number of PV⁺INs was documented in M1 motor cortex in mice of either sex (data not shown). In male mice, TH did not prevent the decline in the number of PV⁺INs (−36% in CA1 and −33% in the CA3 vs. sham, Fig. 2A and Fig. 2B), despite the temporary protection afforded by TH against hippocampal atrophy (Fig 1A₂ and 1B₂). However, in female mice, TH attenuated the deficit in PV⁺INs in CA1 and CA3 (Fig. 2A and B), despite the persistent hippocampal atrophy (Fig 1A₂ and 2B₂). The number of PV⁺INs showed a stronger correlation with histological scores of hippocampal injury (Fig 2C₁ and Fig 2D₁) than with quantification of hippocampal atrophy (Fig 2C₂ and Fig 2D₂) in both CA1 (Fig. 2C) and CA3 (Fig. 2D). No sex dimorphism was identified in these relationships. In the CA1 PCL, counts of PV⁺INs inversely correlated with scores of histological injury of the hippocampus after neonatal HI, equally in males ($R^2 = 0.46$, $p < 0.001$) and female mice ($R^2 = 0.45$, $p < 0.001$, data not shown). In both sexes, the latency to S3 seizure with flurothyl did not correlate with the deficit in PV⁺INs in either CA1 or CA3 (data not shown). However, in male mice, latency to S5 seizure with flurothyl directly correlated with the number of PV⁺INs in the PCL of CA1 ($p = 0.006$, Fig 2E₁) and CA3 ($p = 0.008$, Fig 2F₁). This correlation was non-linear, suggesting a PV-independent mechanism of compensation, preventing higher susceptibility to flurothyl-induced seizures until the PV⁺IN deficit reached an inflexion point (~50 PV⁺INs/mm² in CA1 and ~40 PV⁺INs/mm² in CA3). In female mice, latency to S5 seizure with flurothyl did not correlate with PV⁺IN counts in CA1 (Fig 2E₂) or CA3 (Fig 2F₂). Because hippocampal atrophy 8 days after neonatal HI (Fig. 1D and E) showed a strong correlation with latency to S5, we applied a linear regression model to determine the interaction of the deficit of PV⁺INs with hippocampal atrophy in predicting S5 latency. Only in male mice, did the interaction between PV⁺INs and hippocampal volume better predict S5 latency ($\beta = 0.508$, $p = 0.016$) compared to either of them alone.

Preservation of SST⁺ INs in the hippocampus after neonatal HI did not correlate with flurothyl seizure susceptibility. The soma of SST⁺INs were primarily identified in the oriens layer (OrL) with projection towards PCL on their path thru the radiatum layer (RdL) to the lacunosum moleculare layer (LML) of the CA1 and CA3 subfields (Supplemental Fig. 1). Because of this distribution, we quantified the number of SST⁺INs per mm² as well as the area of SST IR within the combined OrL-PCL region of interest. Unlike the decline in PV⁺INs documented 8 days after HI, the number of SST⁺INs and SST IR were preserved in

CA1 (Supplemental Fig. 2A) and CA3 (Supplemental Fig. 2B). This preservation of SST⁺INs was seen equally in both sexes (data not shown). In contrast with the correlations with PV⁺INs reported above (Fig. 2C and D), the number of SST⁺INs and percent area of SST IR within the OrL-PCL in the CA1 (Supplemental Fig. 2C) and CA3 (Supplemental Fig. 2D) did not correlate with the severity of histological injury of the hippocampus. Thus, even mice demonstrating severe hippocampal injury had preserved SST⁺INs 8 days after neonatal HI. Neither the number of SST⁺INs nor the area of SST IF correlated with seizure latency (data not shown). Since increased expression of NADPH dehydrogenase and nitric oxide synthase (NOS) is mechanistically linked to the preservation of SST⁺INs in neocortex, striatum, and caudate-putamen after neonatal HI in rodents (Beal et al., 1989; Ferrante et al., 1985; Ferriero et al., 1988), we explored if nNOS was increased in SST⁺INs of the hippocampus after neonatal HI. While hippocampal PV⁺ or SST⁺INs of uninjured mice did not co-express nNOS (Supplemental Fig 2E₁), some SST⁺INs became nNOS⁺ 8 days after HI (Supplemental Fig 2E₂).

Few CAL⁺INs were seen in the OrL-PCL layers of the CA1. Unlike PV⁺ and SST⁺INs, few CAL⁺ somas were identified within the OrL-PCL of the CA1 (Supplemental Fig. 3) and none were detected in the CA3 (data not shown). Similarly, the distribution and density of CAL⁺ perisomatic synaptic boutons (Supplemental Fig 3A₂ and 3A₃), and the co-localization with the GABAergic presynaptic marker GAD65/67 (Supplemental Fig 3A₅ and 3A₆), within the CA1 PCL were minimal compared to PV. Neonatal HI appears to change the morphology of CAL⁺INs, which become attritional (Supplemental Fig. 3B). Because the impact neonatal HI in those few CAL⁺INs within the CA1 PCL was deemed to be negligible within the region of interest, we did not pursue further quantification or morphological analysis of CAL⁺INs in these experiments. Of note, CAL IR was intense in other regions of the dorsal hippocampus, such as the LML and afferent bundles within the RdL of CA3 in proximity to CA2 from the DG (Supplemental Fig 3A₃ and 3B₃, arrow).

Decreased GABA_BR in the hippocampus after neonatal HI did not explain flurothyl seizure susceptibility. GABA_B R1 subunit (GABA_BR1) IF within the PCL was decreased by 41% in CA1 (KW ANOVA $p = 0.016$; $p = 0.024$ vs. sham; Fig 3A₁) and 26.3% in CA3 (KW ANOVA $p = 0.011$; $p = 0.019$ vs. sham; Fig 3B₁). Although both males and females showed the same changes, male mice had a greater variability in the GABA_BR1 deficit 8 days after HI, and thus only GABA_BR1 deficits in female mice reached significance in CA1 (KW ANOVA $p = 0.04$; $p = 0.03$ vs. sham) and CA3 (KW ANOVA $p = 0.04$; $p = 0.02$ vs. sham; data not shown). GABA_B R2 subunit (GABA_BR2) also decreased by 57% (KW ANOVA $p = 0.004$; $p = 0.006$ vs. sham, Fig 3C₁) and 40% (KW ANOVA $p = 0.014$; $p = 0.016$ vs. sham, Fig 3D₁) in CA1 and CA3 of NT mice, respectively. No sex dimorphism was observed in the expression of GABA_BR2 (data not shown). TH did not attenuate either GABA_BR1 or R2 deficits 8 days after neonatal HI. The inhibitory effect of the GABA_BR depends on its localization to pre- vs. post-synaptic membranes of INs and PCs. To address this question, we evaluated the relationship between GABA_BR subunit levels and IN counts. GABA_BR1 and R2 areas of IF correlated only weakly with PV⁺INs counts in CA1 (Fig 3A₂ and Fig 3C₂) and CA3 (Fig 3B₂ and Fig 3D₂), thus, loss of PV⁺ inhibitory synapses may only partially explain GABA_BR decrease. Detailed histopathological evaluation showed that both GABA_BR1 and GABA_BR2 were localized marginalized to the membrane of neurons in the

PCL of CA1 (Fig. 3E) and CA3 (Fig. 3F) and their expression was decreased 8 days after HI. However, a small number of cells within the PCL expressed GABA_BR1 in a cytosolic distribution (Fig 3E₃ and 3F₃, insets a). GABA_BR2 did not produce this pattern of IF (Fig 3E₂ and 3F₂). Cells expressing GABA_BR1 on the surface occasionally also expressed PV, but not CAL or SST. In sham mice, PV⁺INs expressed GABA_BR1 and R2 on the membrane (Fig 3E₃ and 3F₃, insets b). Neither GABA_BR1 nor R2 areas of IF correlated with hippocampal atrophy, even following sex stratification (data not shown). Although histological scores of hippocampal injury inversely correlated with GABA_BR1 and R2 areas of IF in CA1 (Fig 3G₁ and 3H₁) and CA3 (Fig 3G₂ and 3H₂), these correlations were modest, more so for GABA_BR1. Lastly, neither GABA_BR1 nor GABA_BR2 correlated with latency to S3 of S5 in males or female mice (data not shown).

Increased GABA_AR α1 subunit IF in CA1 after HI modifies the relationship of PV⁺INs to flurothyl seizure susceptibility. We subsequently investigated changes in the GABA_A receptor (GABA_AR), flurothyl's target. Since PV and SST expressing INs are among the most abundant sources of α1 subunit-containing GABA_ARs, (Gao et al., 1995; Gao and Fritschy, 1994) we specifically focused our experiments on the α1 subunit. GABA_AR α1 subunit (GABA_ARα) increased by 75% in CA1 of NT-treated HI injured mice (KW ANOVA $p = 0.012$; $p = 0.009$ vs. sham; Fig 4A₃ and 4B₁). The increase in GABA_ARα1 8d after HI was similar in both sexes (data not shown). TH attenuated the increase in GABA_ARα1 subunit in CA1 by 65% in male mice (KW ANOVA $p = 0.005$; $p = 0.03$ NT vs. TH; Fig 4B₁), while the attenuation was minimal in female mice (data not shown). GABA_ARα levels correlated inversely with the number of PV⁺INs ($R^2 = 0.29$, $p < 0.001$, Fig 4B₂). Large increases in GABA_ARα1 IF on the order of 3 to 4-fold were observed in some HI-injured mice as shown in Fig 4Ca. A non-linear correlation between hippocampal injury and GABA_ARα1 IF was documented in males ($R^2 = 0.58$, $p < 0.001$) and females ($R^2 = 0.29$, $p = 0.03$; Fig. 4D). Stratification by sex suggested that GABA_ARα1 increase in HI-injured female mice is evident with less severe injury than in male mice. Female mice reached peak GABA_ARα1 IF with hippocampal injury scores of 3 to 4, whereas male mice did not reach the same level of expression until injury scores exceeded 6 (Fig. 4D). Hippocampal atrophy assessed by right hippocampal volume or residual volume correlated inversely with GABA_ARα1 IF in male, but not in female mice (Fig. 4E). Although this sex dimorphism mimics that seen between flurothyl seizure latencies and hippocampal atrophy (Fig. 1D and E) and PV⁺IN deficits (Fig. 2E and F), neither latency to S3 nor S5 seizures correlated with CA1 GABA_ARα1 IF in males (Fig. 4F). Increased expression of post-synaptic GABA_ARs on preserved PV⁺ GABAergic synapses after HI injury may strengthen the inhibitory effect of GABA on the residual PCs. To determine whether this is the case counts of PV⁺INs were adjusted to the GABA_ARα1 expression and the association with seizure susceptibility compared to that achieved by PV⁺IN counts alone. This adjustment simplified the relationship of PV⁺INs with latency to S5 seizure from cubic (Fig 1E₁) to linear in male mice ($R^2 = 0.28$; $p = 0.018$; Fig. 4G). Adjustment had no effect on the non-significant correlations with latency to S3 seizures (data not shown). These findings were only significant in CA1, and not in CA3 (data not shown).

4. Discussion

We report in the hippocampus a novel sex-specific GABA-mediated mechanism of compensation after HI that correlates with flurothyl seizure susceptibility. There is a correlation between flurothyl seizure susceptibility and histological hippocampal injury after neonatal HI that is specific to male mice (McNally et al., 2019). In the same model, we show that flurothyl seizure susceptibility correlates with hippocampal atrophy after neonatal HI in male mice, but similar to histological scoring, it does not fully explain the variability of responses to fluorothyl. The proposed GABA-specific changes after HI include a loss of PV⁺INs with a concurrent increase in GABA_AR α expression. This likely potentiates the inhibitory effect of GABA on PCs, thus decreasing flurothyl seizure susceptibility after HI injury in male mice. These same changes in females are unrelated to flurothyl seizure susceptibility. The presence of this relationship in male mice suggests sexually distinct resilience and response to HI injury in the developing hippocampus. Although the decreased GABA_BR subunit expression and the patterns of GABA_BR subunit staining in PV⁺INs may suggest a role for these receptors in the compensatory mechanism by potentiating inhibitory input, these changes did not correlate with fluorothyl seizure susceptibility. Lastly, hippocampal SST⁺INs appeared to be resistant to neonatal HI in agreement with previously published work (Beal et al., 1989; Ferrante et al., 1985; Ferriero et al., 1988) and were unrelated to later protection from flurothyl seizures in either sex.

These findings are consistent with past work in both rodents and humans showing that neonatal HI gives rise to an inhibitory dysmaturation phenotype due to disruptions in inhibitory system development (Chavez-Valdez et al., 2018; Robinson et al., 2006) and that inhibitory dysmaturation increases susceptibility to seizures later in life (Failor et al., 2010; Le Magueresse and Monyer, 2013; Schwaller et al., 2004). Sex-specific influences on this inhibitory dysmaturation and subsequent seizure susceptibility are not clear, however, previous results show a sexually distinct correlation between hippocampal injury and flurothyl seizure susceptibility after HI (McNally et al., 2019). This and the findings in the current study support the existence of sex-specific differences in pathophysiological mechanisms after neonatal HI that may be explained by sex-specific differences in baseline development of inhibitory systems. There is growing evidence of sex-specific differences in the functional maturation of GABAergic interneurons and receptors and response to injury. In vitro and in vivo evidence shows that females have an earlier maturation of GABA_AR inhibitory signaling than males (Akman et al., 2014; Chavez-Valdez et al., 2018; Galanopoulou, 2008; Giorgi et al., 2014; Nuñez and McCarthy, 2009). There are also sex differences in the GABA_BR signaling during brain development. Its activity pre- and post-synaptically in multiple cortical and subcortical brain regions varies by sex in healthy neonatal rodents (Liu and Herbison, 2011; Marron Fernandez de Valasco et al., 2015). Female mouse pups display more advanced expression of inhibitory PV⁺INs compared to male pups (Chavez-Valdez et al., 2018). Such findings support the existence of distinct baseline sex-differences in the maturation of inhibitory systems in neonatal rodents.

GABA_BRs are G-protein coupled receptors that mediate slow inhibitory responses. Although GABA_BR1 and R2 IF decreased in both sexes in CA1 and CA3 after HI, these decreases correlated only weakly with PV⁺INs counts. Decreased GABA_BR1 and R2

correlated with greater hippocampal injury, but by itself these changes did not explain changes in flurothyl seizure susceptibility. Notably, GABA_BR1 IF revealed two predominant patterns, perikaryal-cytoplasmic and marginalized to the membrane. What these distinct histological patterns reveal about GABA_B internalization needs further study. Although these patterns occur in both the sham and HI CA1 and CA3, it is possible these patterns suggest compensatory mechanisms to preserve inhibitory output. It is possible that i) PV⁺INs have decreased GABA_BR1 and R2 after HI in NT mice or ii) PV⁺INs have preserved GABA_BR2, but increased cytoplasmic GABA_BR1 in TH-treated mice. Either of these events could result in decreased inhibition of release of GABA by PV⁺INs, thus preserving inhibitory output onto PCs and modulating seizure susceptibility. Cytoplasmic localization of the GABA_BR1 may indicate that those INs are better positioned to dynamically mobilize the subunit to the membrane via preserved protein trafficking systems (Doly et al., 2016). Further in depth evaluations of GABA_BR expression, localization, and physiological function are needed to understand its role in seizure susceptibility.

GABA_ARs are heterogenous pentamers composed of varying combinations of 16 subunits with cellular and regional specificity in the brain. Notably, GABA_ARs containing the $\alpha 1$ subunit are the most abundantly expressed in the brain (Olsen and Sieghart, 2009). In the hippocampus, $\alpha 1$ subunit containing GABA_ARs cluster on the post-synaptic membrane of GABAergic synapses targeting the soma and dendrites of PCs, where they exert fast inhibition (Gao and Fritschy, 1994; Olsen and Sieghart, 2009). Increase in CA1 GABA_AR $\alpha 1$ occurs after juvenile stress (Ardi et al., 2019); however changes linked to neonatal HI were unknown. In the present study, we found that GABA_AR $\alpha 1$ IF increased after HI in both sexes. It is possible that this increase may be a reaction to the deficits in PV⁺INs (Chavez-Valdez et al., 2018). However, sexually distinct patterns of response were observed in our model. Injured females showed an increase in GABA_AR $\alpha 1$ in CA1 at lower hippocampal injury scores than injured males, but that increase did not correlate with hippocampal atrophy or latency to S3 or S5 seizures with flurothyl exposure. In contrast to males, females do not appear to be equally protected by TH after HI injury with respect to hippocampal atrophy. However, TH does provide partial protection against PV⁺IN deficits in females with simultaneous preservation of the compensatory GABA_AR $\alpha 1$ increase after injury. In females, the increase in GABA_AR $\alpha 1$ may adequately compensate for the remaining PV⁺IN deficits and, thus, prevent significant changes in flurothyl seizure susceptibility. In contrast, injured males required greater severity of hippocampal injury to reach the same levels of GABA_AR $\alpha 1$ upregulation as females. Unlike females, the greater injury in males correlated inversely with hippocampal volumes. While no direct correlation between GABA_AR $\alpha 1$ levels and flurothyl seizure latencies were seen in males, adjusting PV⁺IN counts for levels of GABA_AR $\alpha 1$ in the CA1 improved the correlation with flurothyl seizure susceptibility. It is possible that increased expression of post-synaptic GABA_ARs on preserved PV⁺IN GABAergic synapses after HI injury may strengthen the inhibitory effect of GABA on the residual PCs. As a consequence, these changes may modulate susceptibility to flurothyl-induced seizures. Notably, the increased GABA_AR $\alpha 1$ concentrations remain insufficient to compensate for the PV⁺IN deficit to protect against flurothyl seizures with more significant HC injury.

The findings of hippocampal atrophy in the current study are consistent with our previously published results (Burnsed et al., 2015). Interestingly, we show that histology scores correlate better with PV⁺IN deficits than with hippocampal volumes, and this may explain why other methods of injury assessment such as changes in area did not correlate with PV + INs deficits in our past work (Chavez-Valdez et al., 2018). The methodology in the current study does present limitations that we have taken into consideration while interpreting our results. Immunohistochemistry permits only indirect measurements of correlation without definitive localization of proteins and does not allow determination of causation. We did not directly measure the inhibitory output capacity of our system. Additionally, assessing seizure susceptibility to a chemo-convulsant has limits in terms of clinical translatability and additional methods of seizure induction are necessary to validate our findings. However, our results do demonstrate important relationships between hippocampal injury, GABAergic systems, and seizure susceptibility that may have important clinical ramifications.

We conclude that changes in the hippocampal GABAergic circuit may provide seizure susceptibility compensation after HI injury. This may allow male mice to retain flurothyl seizure protection after HI, but only up to a certain threshold after which the injury is too great to allow such a compensation. Future work should aim to measure direct function of this compensatory mechanism in addition to testing whether this injury threshold in male mice is fixed or variable. Finally, translational research into treatments for seizures after neonatal HI that utilize drugs that target components of this compensatory mechanism could prove fruitful and studies need to be powered to detect sex differences in response to treatment.

Supplementary Material

Refer to Web version on PubMed Central for supplementary material.

Acknowledgements

The authors thank Mrs. Deborah Flock for her technical support and Mrs. Rosie Silva for her administrative assistance

Funding Acknowledgements

This work has been supported by the National Institutes of Health (KO8NS096115, 3K08NS096115-03S1 – RC-V; RO1HD070996, RO1HD086058, R21AG061643 – FJN; R25NS065729 – MAM; KO8NS097704 – RJF.), the JHU-SOM Clinician Scientist Award - RC-V

Abbreviations:

CA	cornu ammonis
CAL	calretinin
DAPI	4',6-diamidino-2-phenylindole
DG	dentate gyrus
GABA	gamma-aminobutyric acid

GABA_ARα1	GABA _A receptor α 1 subunit
GABA_BR	GABA _B receptor
GCL	granular cell layer
GFAP	glial fibrillary acidic protein
HI	hypoxic-ischemic brain injury
IF	immunofluorescence
IHC	immunohistochemistry
IN	interneuron
LML	lacunosum moleculare layer
NGS	normal goat serum
NOS	nitric oxide synthase
NT	normothermia
OrL	oriens layer
P	postnatal day
PCL	pyramidal cell layer
PV	parvalbumin
RdL	radiatum layer
S3	stage 3 seizure
S5	stage 5 seizure
SST	somatostatin
TBS-T	0.1% Tween/TBS
TH	therapeutic hypothermia
WB	western blot

References

- Akman O, Moshé SL, Galanopoulou AS, 2014 Sex-specific consequences of early life seizures. *Neurobiol. Dis.* 72 (Pt B), 153–166. 10.1016/j.nbd.2014.05.021. [PubMed: 24874547]
- Annink KV, de Vries LS, Groenendaal F, van den Heuvel MP, van Haren NEM, Swaab H, van Handel M, Jongmans MJ, Benders MJ, van der Aa NE, 2019 The long-term effect of perinatal asphyxia on hippocampal volumes. *Pediatr. Res.* 85, 43–49. 10.1038/s41390-018-0115-8. [PubMed: 30254237]
- Ardi Z, Richter-Levin A, Xu L, Cao X, Volkmer H, Stork O, Richter-Levin G, 2019 The role of the GABA_A receptor alpha 1 subunit in the ventral hippocampus in stress resilience. *Sci. Rep.* 9, 1–11. 10.1038/s41598-019-49824-4. [PubMed: 30626917]

- Azzopardi DV, Strohm B, Edwards AD, Dyet L, Halliday HL, Juszczak E, Kapellou O, Levene M, Marlow N, Porter E, Thoresen M, Whitelaw A, Brocklehurst P, 2009 Moderate hypothermia to treat perinatal Asphyxial encephalopathy. *N. Engl. J. Med.* 361, 1349–1358. 10.1056/NEJMoa0900854. [PubMed: 19797281]
- Bassan H, Bental Y, Shany E, Berger I, Froom P, Levi L, Shiff Y, 2008 Neonatal seizures: dilemmas in workup and management. *Pediatr. Neurol.* 38, 415–421. 10.1016/j.pediatrneurol.2008.03.003. [PubMed: 18486824]
- Beal MF, Kowall NW, Swartz KJ, Ferrante RJ, Martin JB, 1989 Differential sparing of somatostatin-neuropeptide y and cholinergic neurons following striatal excitotoxin lesions. *Synapse* 3, 38–47. 10.1002/syn.890030106. [PubMed: 2563916]
- Bittigau P, Sifringer M, Ikonomidou C, 2003 Antiepileptic drugs and apoptosis in the developing brain, in: *annals of the new York Academy of Sciences.* Ann N Y Acad Sci. 993, 103–114. 10.1111/j.1749-6632.2003.tb07517.x. [PubMed: 12853301]
- Boylan GB, Kharoshankaya L, Wusthoff CJ, 2015 Seizures and hypothermia: importance of electroencephalographic monitoring and considerations for treatment. *Semin. Fetal Neonatal Med.* 20, 103–108. 10.1016/j.siny.2015.01.001. [PubMed: 25683598]
- Bradford MM, 1976 A rapid and sensitive method for the quantitation of microgram quantities of protein utilizing the principle of protein-dye binding. *Anal. Biochem.* 72, 248–254. 10.1016/0003-2697(76)90527-3. [PubMed: 942051]
- Burnsed JC, Chavez-Valdez R, Hossain MS, Kesavan K, Martin LJ, Zhang J, Northington FJ, 2015 Hypoxia-ischemia and therapeutic hypothermia in the neonatal mouse brain - a longitudinal study. *PLoS One* 10, 1–20. 10.1371/journal.pone.0118889.
- Chavez-Valdez R, Emerson P, Goffigan-Homes J, Kirkwood A, Martin LJ, Northington FJ, 2018 Delayed injury of hippocampal interneurons after neonatal hypoxia-ischemia and therapeutic hypothermia in a murine model. *Hippocampus* 28, 617–630. 10.1002/hipo.22965. [PubMed: 29781223]
- Chavez-Valdez R, Lechner C, Emerson P, Northington FJ, Martin LJ, 2020 Accumulation of PSA-NCAM marks nascent neurodegeneration in the dorsal hippocampus after neonatal hypoxic-ischemic brain injury in mice. *J. Cereb. Blood Flow Metab.* 10.1177/0271678X20942707.
- Clancy RR, 2006 Summary proceedings from the neurology group on neonatal seizures. *Pediatrics* 117, 23–27.
- Diaz J, Abiola S, Kim N, Avaritt O, Flock D, Yu J, Northington FJ, Chavez-Valdez R, 2017 Therapeutic hypothermia provides variable protection against behavioral deficits after neonatal hypoxia-ischemia: a potential role for brain-derived neurotrophic factor. *Dev. Neurosci.* 39, 257–272. 10.1159/000454949. [PubMed: 28196356]
- Doly S, Shirvani H, Gta G, Meye FJ, Emerit MB, Enslin H, Achour L, Pardo-Lopez L, Yang SK, Armand V, Gardette R, Giros B, Gassmann M, Bettler B, Mameli M, Darmon M, Marullo S, 2016 GABA B receptor cell-surface export is controlled by an endoplasmic reticulum gatekeeper. *Mol. Psychiatry* 21, 480–490. 10.1038/mp.2015.72. [PubMed: 26033241]
- Failor S, Nguyen V, Darcy DP, Cang J, Wendland MF, Stryker MP, McQuillen PS, 2010 Neonatal cerebral hypoxia–ischemia impairs plasticity in rat visual cortex. *J. Neurosci.* 30, 81–92. 10.1523/JNEUROSCI.5656-08.2010. [PubMed: 20053890]
- Ferrante RJ, Kowall NW, Beal MF, Richardson EP, Bird ED, Martin JB, 1985 Selective sparing of a class of striatal neurons in Huntington’s disease. *Science* 230, 561–563. 10.1017/CBO9781107415324.004. [PubMed: 2931802]
- Ferriero DM, Arcavi LJ, Sagar SM, McIntosh TK, Simon RP, 1988 Selective sparing of NADPH-diaphorase neurons in neonatal hypoxia-ischemia. *Ann. Neurol.* 24, 670–676. 10.1002/ana.410240512. [PubMed: 2904792]
- Gadian DG, Aicardi J, Watkins KE, Porter DA, Mishkin M, Vargha-Khadem F, 2000 Developmental amnesia associated with early hypoxic-ischaemic injury. *Brain* 123, 499–507. 10.1093/brain/123.3.499. [PubMed: 10686173]
- Galanopoulou AS, 2008 Dissociated gender-specific effects of recurrent seizures on GABA signaling in CA1 pyramidal neurons: role of GABAA receptors. *J. Neurosci.* 28, 1557–1567. 10.1523/JNEUROSCI.5180-07.2008. [PubMed: 18272677]

- Gao B, Fritschy JM, 1994 Selective allocation of GABAA receptors containing the $\alpha 1$ subunit to Neurochemically distinct subpopulations of rat hippocampal interneurons. *Eur. J. Neurosci.* 6, 837–853. 10.1111/j.1460-9568.1994.tb00994.x. [PubMed: 8075825]
- Gao B, Hornung J-P, Fritschy J, 1995 Identification of distinct GABAA-receptor subtypes in cholinergic and parvalbumin-positive neurons of the rat and marmoset medial septum - diagonal band complex. *Neuroscience* 65, 101–117. 10.1016/0306-4522(94)00480-s. [PubMed: 7753393]
- Giorgi FS, Galanopoulou AS, Moshé SL, 2014 Sex dimorphism in seizure-controlling networks. *Neurobiol. Dis.* 72, 144–152. 10.1016/j.nbd.2014.05.010. [PubMed: 24851800]
- Glass HC, Glidden D, Jeremy RJ, Barkovich AJ, Ferriero DM, Miller SP, 2009 Clinical neonatal seizures are independently associated with outcome in infants at risk for hypoxic-ischemic brain injury. *J. Pediatr.* 155, 318–323. 10.1016/j.jpeds.2009.03.040. [PubMed: 19540512]
- Glass HC, Wusthoff CJ, Shellhaas RA, Tsuchida TN, Bonifacio SL, Cordeiro M, Sullivan J, Abend NS, Chang T, 2014 Risk factors for EEG seizures in neonates treated with hypothermia: a multicenter cohort study. *Neurology* 82, 1239–1244. 10.1212/WNL.0000000000000282. [PubMed: 24610326]
- Glass HC, Soul JS, Chu CJ, Massey SL, Wusthoff CJ, Chang T, Cilio MR, Bonifacio SL, Abend NS, Thomas C, Lemmon M, McCulloch CE, Shellhaas RA, 2019 Response to antiseizure medications in neonates with acute symptomatic seizures. *Epilepsia* 60, e20–e24. 10.1111/epi.14671. [PubMed: 30790268]
- Goffigan-Holmes J, Sanabria D, Diaz J, Flock D, Chavez-Valdez R, 2019 Calbindin-1 expression in the Hippocampus following neonatal hypoxia-ischemia and therapeutic hypothermia and deficits in spatial memory. *Dev Neurosci.* 12, 1–15. 10.1159/000497056.
- Graham EM, Sheldon RA, Flock DL, Ferriero DM, Martin LJ, O’Riordan DP, Northington FJ, 2004 Neonatal mice lacking functional Fas death receptors are resistant to hypoxic-ischemic brain injury. *Neurobiol. Dis.* 17, 89–98. 10.1016/j.nbd.2004.05.007. [PubMed: 15350969]
- Hellström-Westas L, Boylan G, Ågren J, 2015 Systematic review of neonatal seizure management strategies provides guidance on anti-epileptic treatment. *Acta Paediatr. Int. J. Paediatr.* 104, 123–129. 10.1111/apa.12812.
- Kurinczuk JJ, White-Koning M, Badawi N, 2010 Epidemiology of neonatal encephalopathy and hypoxic-ischaemic encephalopathy. *Early Hum. Dev.* 86, 329–338. 10.1016/j.earlhumdev.2010.05.010. [PubMed: 20554402]
- Le Magueresse C, Monyer H, 2013 GABAergic interneurons shape the functional maturation of the cortex. *Neuron* 77, 388–405. 10.1016/j.neuron.2013.01.011. [PubMed: 23395369]
- Liu X, Herbison AE, 2011 Estrous cycle- and sex-dependent changes in pre- and postsynaptic GABA B control of GnRH neuron excitability. *Endocrinology* 152, 4856–4864. 10.1210/en.2011-1369. [PubMed: 21971155]
- Luhmann HJ, Kirischuk S, Sinning A, Kilb W, 2014 Early GABAergic circuitry in the cerebral cortex. *Curr. Opin. Neurobiol.* 26, 72–78. 10.1016/j.conb.2013.12.014. [PubMed: 24434608]
- Markovic SN, Murasko DM, 1993 Anesthesia inhibits interferon-induced natural killer cell cytotoxicity via induction of CD8+ suppressor cells. *Cell. Immunol.* 151, 474–480. 10.1006/cimm.1993.1256. [PubMed: 8402951]
- Marron Fernandez de Valasco E, Hearing M, Xia Z, Victoria NC, Lujan R, Wickman K, 2015 Sex differences in GABABR-GIRK signaling in layer 5/6 pyramidal neurons of the mouse prelimbic cortex. *Neuropharmacology* 95, 353–360. 10.1016/j.neuropharm.2015.03.029. [PubMed: 25843643]
- McBride MC, Laroia N, Guillet R, 2000 Electrographic seizures in neonates correlate with poor neurodevelopmental outcome. *Neurology* 55, 506–513. 10.1212/WNL.55.4.506. [PubMed: 10953181]
- McNally MA, Hartman AL, 2017 Variability in preferred Management of Electrographic Seizures in neonatal hypoxic ischemic encephalopathy. *Pediatr. Neurol.* 77 10.1016/j.pediatrneurol.2017.06.006.
- McNally MA, Chavez-Valdez R, Felling RJ, Flock DL, Northington FJ, Stafstrom CE, 2019 Seizure susceptibility correlates with brain injury in male mice treated with hypothermia after neonatal hypoxia-ischemia. *Dev. Neurosci.* 28, 1–10. 10.1159/000496468.

- Mishchenko Y, Hu T, Spacek J, Mendenhall J, Harris KM, Chklovskii DB, 2010 Ultrastructural analysis of hippocampal neuropil from the connectomics perspective. *Neuron* 67, 1009–1020. 10.1016/j.neuron.2010.08.014. [PubMed: 20869597]
- Núñez JL, McCarthy MM, 2009 Resting intracellular calcium concentration, depolarizing gamma-aminobutyric acid and possible role of local estradiol synthesis in the developing male and female hippocampus. *Neuroscience* 158, 623–634. 10.1016/j.neuroscience.2008.09.061. [PubMed: 19007865]
- Olsen RW, Sieghart W, 2009 GABAA receptors: subtypes provide diversity of function and pharmacology. *Neuropharmacology* 56, 141–148. 10.1016/j.neuropharm.2008.07.045. [PubMed: 18760291]
- Painter MJ, Scher MS, Stein AD, Armatti S, Wang Z, Gardiner JC, Paneth N, Minnigh B, Alvin J, 1999 Phenobarbital compared with phenytoin for the treatment of neonatal seizures. *N Engl J Med*. 341, 485–489. 10.1056/NEJM199908123410704. [PubMed: 10441604]
- Pfister RH, Soll RF, 2010 Hypothermia for the treatment of infants with hypoxic-ischemic encephalopathy. *J. Perinatol.* 30, S82–S87. 10.1038/jp.2010.91. [PubMed: 20877413]
- Prichard J, Gallagher B, Glaser G, 1969 Experimental seizure-threshold testing with flurothyl. *J. Pharmacol. Exp. Ther.* 166, 170–178. [PubMed: 5776021]
- Racine RJ, 1972 Modification of seizure activity by electrical stimulation II. Motor seizure. *Electroencephalogr. Clin. Neurophysiol.* 32, 281–294. 10.1016/0013-4694(72)90177-0. [PubMed: 4110397]
- Robinson S, Li Q, DeChant A, Cohen ML, 2006 Neonatal loss of γ -aminobutyric acid pathway expression after human perinatal brain injury. *J. Neurosurg.* 104, 396–408. 10.3171/ped.2006.104.6.396. [PubMed: 16776375]
- Schwaller B, Tetko IV, Tandon P, Silveira DC, Vreugdenhil M, Henzi T, Potier MC, Celio MR, Villa AEP, 2004 Parvalbumin deficiency affects network properties resulting in increased susceptibility to epileptic seizures. *Mol. Cell. Neurosci.* 25, 650–663. 10.1016/j.mcn.2003.12.006. [PubMed: 15080894]
- Schwenk J, Pérez-Garci E, Schneider A, Kollwe A, Gauthier-Kemper A, Fritzius T, Raveh A, Dinamarca MC, Hanuschkin A, Bildl W, Klingauf J, Gassmann M, Schulte U, Bettler B, Fakler B, 2016 Modular composition and dynamics of native GABAB receptors identified by high-resolution proteomics. *Nat. Neurosci.* 19, 233–242. 10.1038/nn.4198. [PubMed: 26691831]
- Shah DK, Wusthoff CJ, Clarke P, Wyatt JS, Ramaiah SM, Dias RJ, Becher J, Kapellou O, Boardman JP, 2014 Electrographic Seizures Are Associated with Brain Injury in Newborns Undergoing Therapeutic Hypothermia 219–225. *Arch Dis Child Fetal Neonatal Ed.* 99, F219–F224. 10.1136/archdischild-2013-305206. [PubMed: 24443407]
- Sheldon RA, Jiang X, Francisco C, Christen S, Vexler ZS, Täuber MG, Ferriero DM, 2004 Manipulation of antioxidant pathways in neonatal murine brain. *Pediatr. Res.* 56, 656–662. 10.1203/01.PDR.0000139413.27864.50. [PubMed: 15295091]
- Shetty J, 2015 Neonatal seizures in hypoxic-ischaemic encephalopathy - risks and benefits of anticonvulsant therapy. *Dev. Med. Child Neurol.* 57, 40–43. 10.1111/dmcn.12724. [PubMed: 25800491]
- Srinivasakumar P, Zempel J, Trivedi S, Wallendorf M, Rao R, Smith B, Inder T, Mathur AM, 2015 Treating EEG seizures in hypoxic ischemic encephalopathy: a randomized controlled trial. *Pediatrics* 136, e1302–e1309. 10.1542/peds.2014-3777. [PubMed: 26482675]
- Sulzbacher S, Farwell JR, Temkin N, Lu AS, Hirtz DG, 1999 Late cognitive effects of early treatment with phenobarbital. *Clin Pediatr* 38, 387–394. 10.1177/000992289903800702.
- Toet MC, Groenendaal F, Osredkar D, Van Huffelen AC, De Vries LS, 2005. Postneonatal epilepsy following amplitude-integrated EEG-detected neonatal seizures. *Pediatr. Neurol.* 32, 241–247. 10.1016/j.pediatrneurol.2004.11.005. [PubMed: 15797180]
- Van Rooij LGM, Van Den Broek MPH, Rademaker CMA, De Vries LS, 2013 Clinical management of seizures in newborns: diagnosis and treatment. *Pediatr. Drugs* 15, 9–18. 10.1007/s40272-012-0005-1.

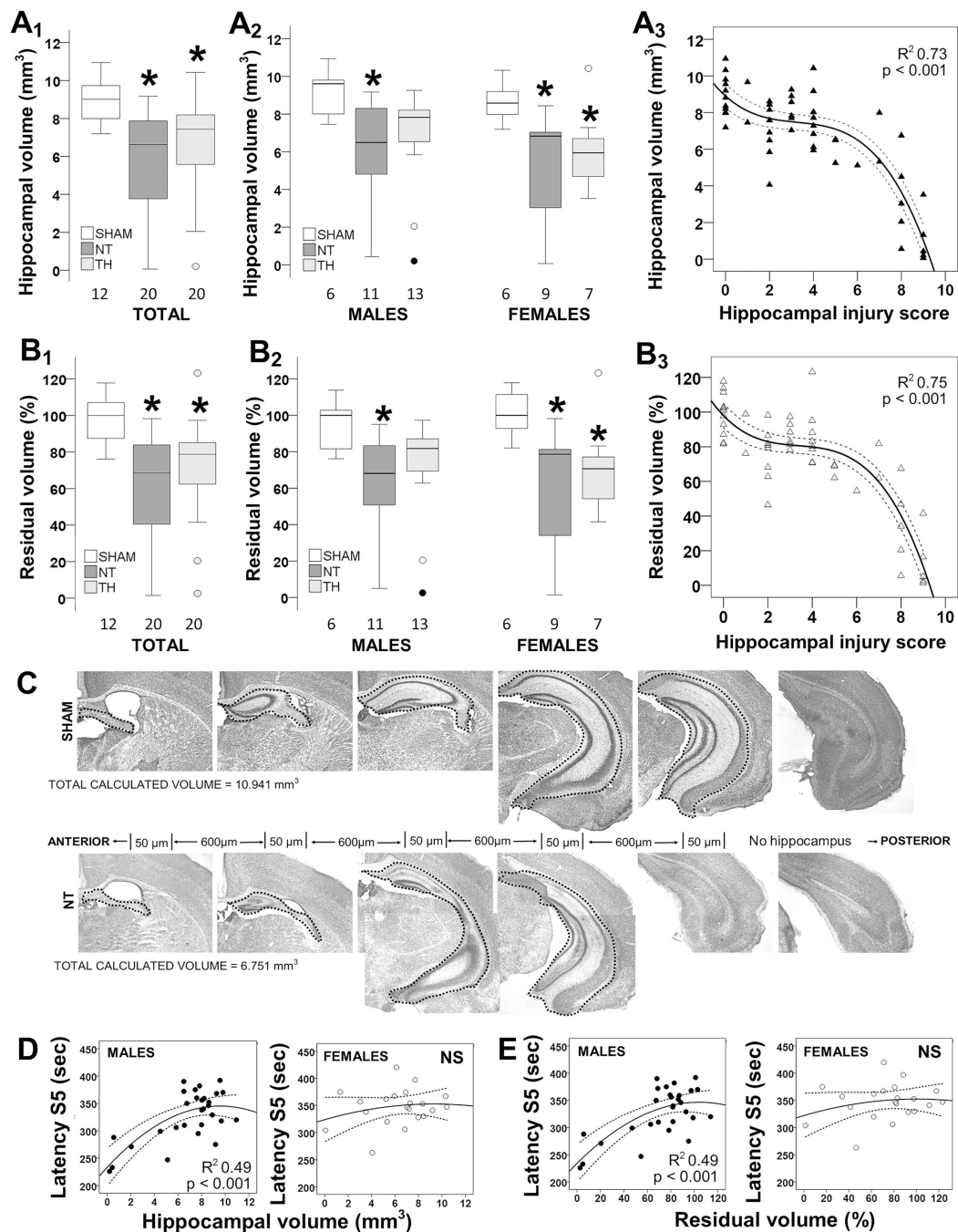


Fig. 1. Correlation between hippocampal atrophy after neonatal hypoxia-ischemia (HI) and seizure susceptibility. Hippocampal volume (A) and residual volume (B) are decreased in mice exposed to HI and normothermia (NT) and this decrease is attenuated by TH (A₁, B₁), which is sexually dimorphic (A₂, B₂). Results are shown as box and whisker plots, where the box is limited by the 25th and 75th percentiles (interquartile range, IQR) and the solid line represents the median. The whiskers are limited by the last data point within 1.5 times the IQR from the median, with outliers included. Kruskal–Wallis ANOVA with Dunn–Bonferoni

post-hoc testing for pair analysis was applied. *, $p < 0.05$. The relationship between hippocampal volumes and histological injury scores is not linear (A₃, B₃). Representative photomicrographs are shown demonstrating hippocampal volume measurements (C). Hippocampal volumes and residual volumes correlated directly with latency to S5 in male mice (D, E). The continuous lines represent the fitted line derived from a non-linear regression and the discontinuous lines represent the 95% confidence boundaries.

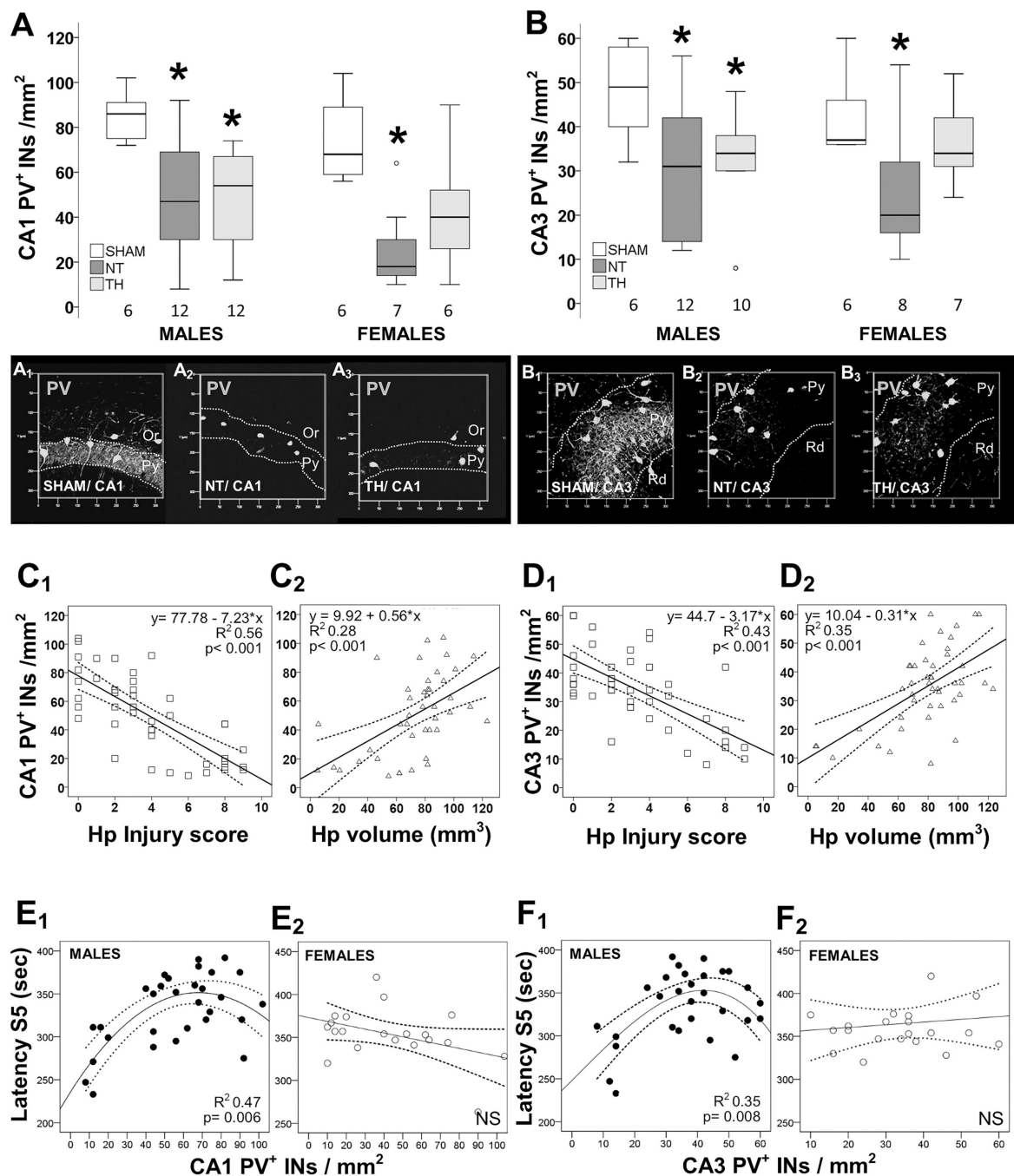


Fig. 2. Sex-specific correlation between number of PV⁺INs, hippocampal injury, and flurothyl seizure susceptibility. Box and whisker plots represent the number of PV⁺INs per mm² in male and female mice sham vs. HI injured treated with normothermia (NT) or therapeutic hypothermia (TH) within the CA1 (A) and CA3 (B) pyramidal cell layers (PCLs). Boxes are limited by the 25th and 75th percentiles (interquartile range, IQR) and whiskers are limited by the last data point within 1.5 times the IQR from the median (continuous line inside the box), with outliers included. Kruskal–Wallis ANOVA with Dunn-Bonferoni post-hoc testing

for pair analysis was applied. *, $p < 0.05$. Representative transparent rendering obtained from z-stack captured at 20×/0.8 objective are shown for CA1 (A₁₋₃) and CA3 (B₁₋₃) hippocampal subfield. Pyramidal (Py), oriens (Or), and radiatum (Rd) layers are labeled. The number of PV⁺INs showed a stronger correlation with histological scores of hippocampal injury (C₁, D₁) than with quantification of hippocampal atrophy (C₂, D₂) in both CA1 (C) and CA3 (D). The correlations between the number of PV⁺INs in hippocampal CA1 (E) and CA3 (F) with latency to S5 seizures are shown for male (E₁, F₁) and female (E₂, F₂) mice. The continuous lines represent the fitted line derived from regression modeling and the discontinuous lines represent the 95% confidence intervals.

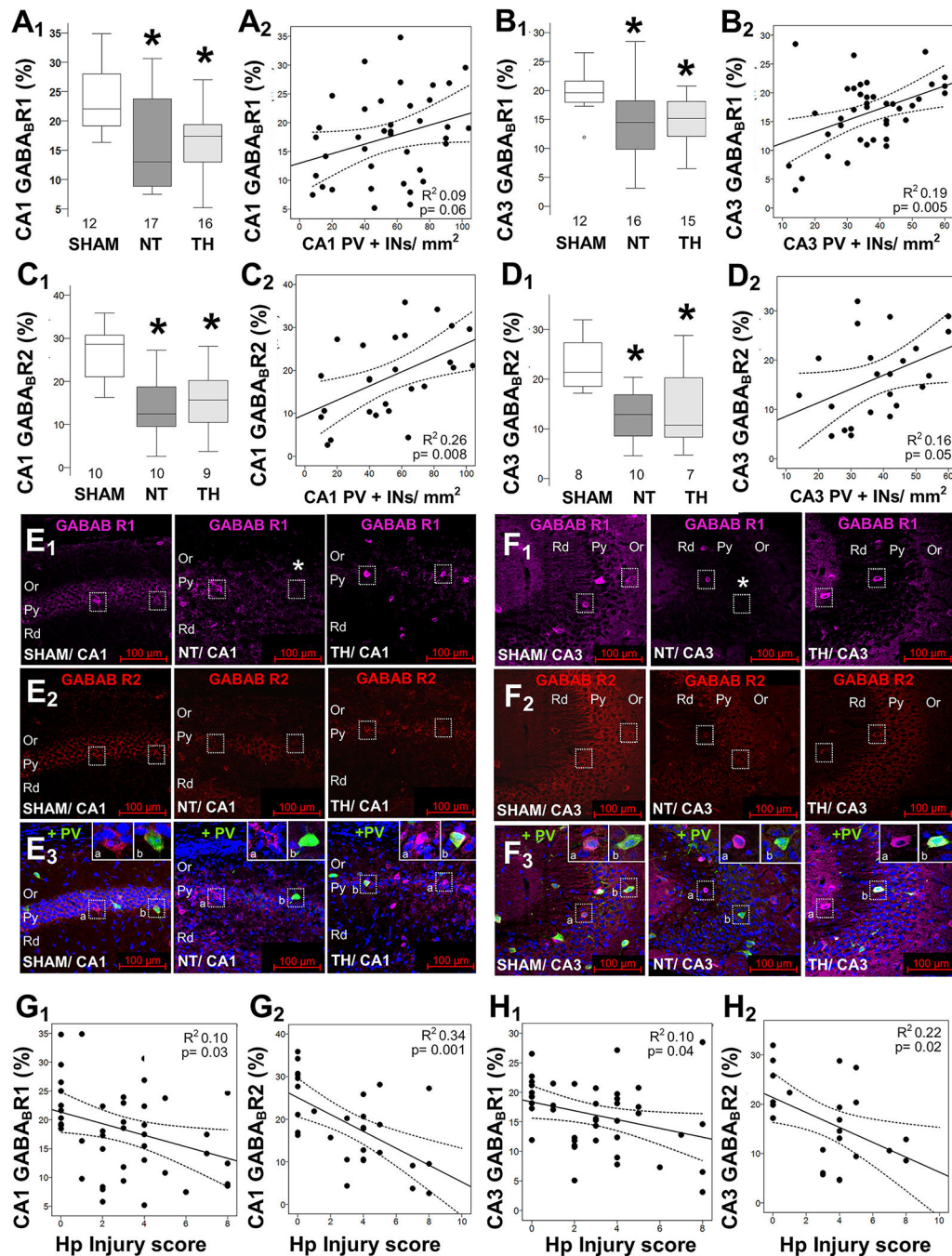


Fig. 3. Decreased GABA_B receptor subunits in the hippocampus after neonatal HI. HI decreases GABA_B R1 subunit (GABA_BR1; A, B) and GABA_B R2 subunit (GABA_BR2; C, D) percent area of expression within the PCL of the CA1 (A₁, C₁) and CA3 (B₁, D₁). No sexual dimorphism was identified (data not shown). Boxes are limited by the 25th and 75th percentiles (interquartile range, IQR) and whiskers are limited by the last data point within 1.5 times the IQR from the median (continuous line inside the box), with outliers included. Kruskal–Wallis ANOVA with Dunn–Bonferoni post-hoc testing for pair analysis was

applied. *, $p < 0.05$. The correlations between the number of PV⁺INs in hippocampal CA1 (A₂, C₂) and CA3 (B₂, D₂) with GABA_BR1 (A₂, B₂) and GABA_BR2 (C₂, D₂) are shown. Representative images from GABA_BR1 (Alexa 647, magenta) and GABA_BR2 (Alexa 568, red) combined with PV (Alexa 488, green) and nuclear stain with DAPI (blue) in merged image, were captured at 20×/0.8 objective to show the CA1 (E) and CA3 (F) hippocampal pyramidal (Py), oriens (Or), and radiatum (Rd) layers. GABA_BR1 and GABA_BR2 levels correlate with hippocampal injury scores in CA1 (G_{1,2}) and CA3 (H_{1,2}). The continuous lines represent the fitted line derived from a linear regression and the discontinuous lines represent the 95% confidence intervals. Sex-stratified and non-stratified correlations with fluorothyl susceptibility were non-significant (data not shown).

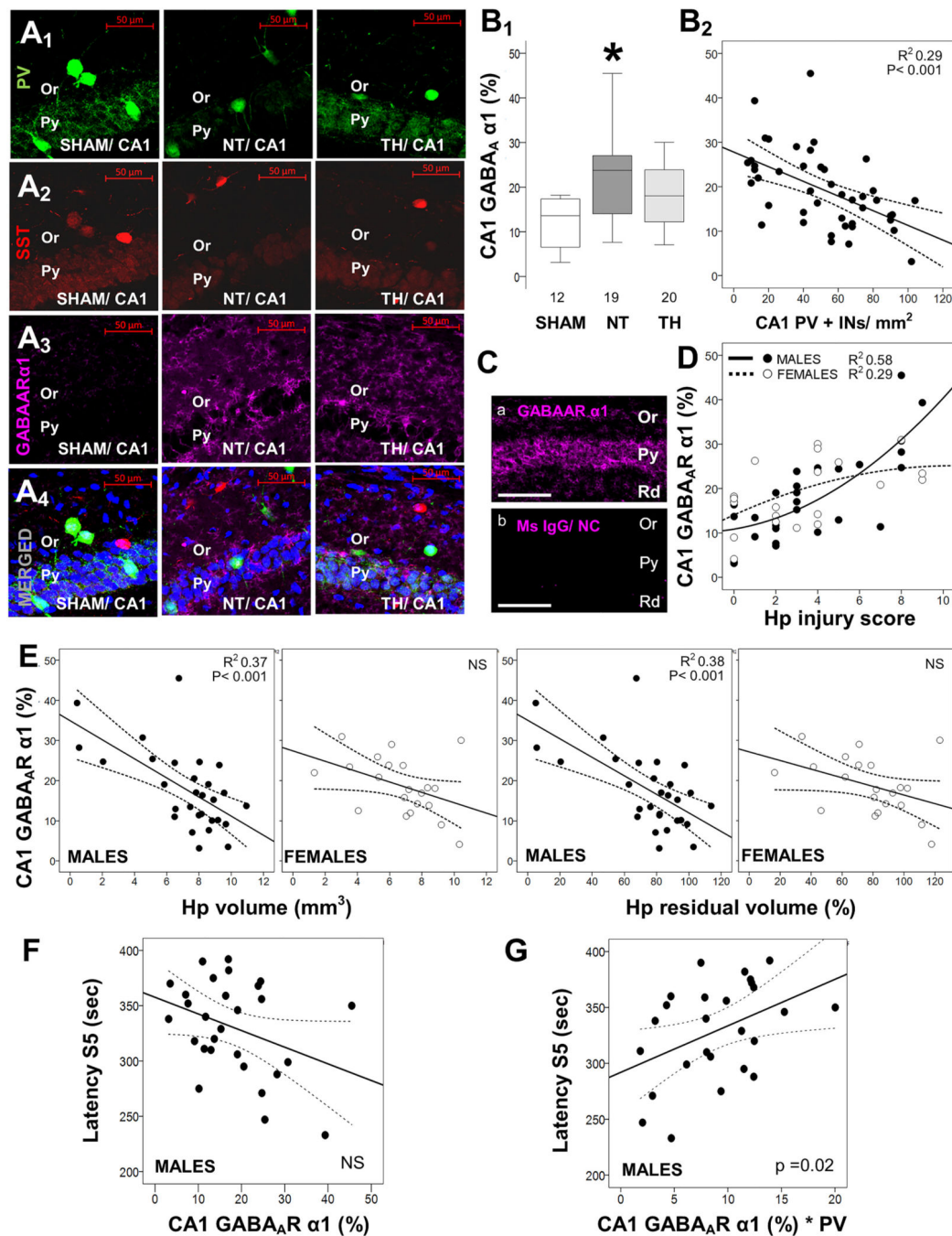


Fig. 4. Increased hippocampal levels of GABA α receptor α 1 subunit correlate with flurothyl seizure susceptibility. Shown are representative confocal images (20 \times /0.8 objective) of hippocampal pyramidal (Py) and oriens (Or) layers for PV (Alexa 488, green; A₁), somatostatin (SST, Alexa 568, red; A₂), GABA α receptor α 1 subunit (GABA α R α 1, Alexa 647, magenta; A₃), and merged (A₄) with nuclear DAPI (blue) in sham, normothermia (NT), and therapeutic hypothermia (TH) mice. Box and whisker plots demonstrate the percent expression of GABA α R α 1 in each group (B₁) and the correlations with the number of PV⁺

interneurons (INs) in the CA1 region (B_2). In some instances, $GABA_A\alpha 1$ immunoreactivity was extreme despite blocking methods (C_a) and absent of non-specific staining in negative controls (C_b). Correlations between $GABA_A\alpha 1$ and hippocampal (Hp) injury scores (D), Hp volume measurements (E), and latency to stage 5 (S5) seizures with flurothyl (F) are shown. Adjustment of the number of PV^+ INs by their relative expression of $GABA_A\alpha 1$ affects the correlation with latency to S5 seizures with flurothyl (G), now becoming linear. Boxes are limited by the 25th and 75th percentiles (interquartile range, IQR) and whiskers are limited by the last data point within 1.5 times the IQR from the median (continuous line inside the box), with outliers included. Kruskal–Wallis ANOVA with Dunn-Bonferoni post-hoc testing for pair analysis was applied. *, $p < 0.05$. In correlation charts, the continuous lines represent the fitted line derived from regression modeling and the discontinuous lines represent the 95% confidence boundaries.